Probabilistic Seismic Hazard Assessments for Northern Southeast Asia

T. Ornthammarath,[a], P. Warnitchai,[b] , C.-H. Chan, [c] , Y. Wang, [c] , X. Shi, [c] , P. H. Nguyen,[d] , L. M. Nguyen [d] , S. Kosuwan,[e] , M. Thant,[f] and K. Sieh [c]

[a] Department of Civil and Environmental Engineering, Mahidol University, Thailand

[b] Civil and Infrastructure Engineering Department, Asian Institute of Technology, Thailand

[c] Earth Observatory of Singapore, Nanyang Technological University, Singapore

[d] Institute of Geophysics, Vietnam Academy of Science and Technology, Vietnam

[e] Active Fault Research Division, Department of Mineral Resources, Thailand

[f] Myanmar Earthquake Committee, Myanmar

Abstract

We present the evaluation of the 2018 Northern Southeast Asia Seismic Hazard Model (NSAHM18) based on combination of smoothed seismicity, subduction zone, and fault models. The smoothed seismicity is used to model observed distributed seismicity from largely unknown sources in current study area. In addition, due to short instrumental earthquake catalog, slip rate and characteristic earthquake magnitudes are incorporated through fault model. In order to achieve this objective, the compiled earthquake catalog and updated active fault database in this region were reexamined and mutually decided to utilize these input parameters. To take into account epistemic uncertainty, logic tree analysis has been implemented incorporating basic quantities such as different three tectonic regions ground-motion models (GMMs) for Shallow Active, Subduction Interface, and Subduction Intraslab, maximum magnitude, and earthquake magnitude frequency relationships. The seismic hazard results are presented in peak ground acceleration maps at 475 and 2475 year return periods.

Keywords: Seismic hazard, Northern Southeast Asia, Probabilistic seismic hazard analysis, Ground motion, Active fault.

1. Introduction

Northern Southeast Asia (NSA) (or Indochina) is an area of highly diverse seismic hazard, from high seismic hazard related to Indo-Australian and Eurasian collision plate boundary including the Myanmar oblique subduction zone to the west, and the relatively low and sparse observed seismicity inside Sundaland plate to the east. Nevertheless, historical damaging earthquakes are also reported inside NSA. Several existing PSHA maps in this region had been published in the past few decades based on the Cornell (1968) [1] approach with different methodologies such as the uniform seismicity rate with different delineated conventional seismic source zone (e.g. Vietnam, Phoung, 1991 [2]; Global, Shedlock et al., 2000 [3]; Myanmar, Myo Thant et al., 2012)[4], or the smoothed seismicity methodology proposed by Frankel (1995) (i.e. Thailand, Ornthammarath et al., 2011) [5]. However, these hazard maps have generally been computed to develop national seismic design code with limited discussion among neighboring countries what should be appropriated fault parameters resulting in different estimated seismic hazard values particularly between national boundaries.

The NSAHM18 is a collaborative effort to overcome the limitation of national borders in this region. It is the regional contribution to the “Global Earthquake Model” initiative to get the consensus of relevant key persons in that region regarding to current data and stage of knowledge. In order to achieve this objective, relevant earthquake database and updated active fault database in this region were reexamined and mutually decided to utilize these input parameters. The original fault parameters using in this study were referred to previous studies by Chan et al. (2017) [6] Additional fault parameters in Thailand are also provided by the Department of Mineral Resources (DMR) presented this newly compiled regional fault database using in current study.

2. EARTHQUAKE CATALOG

In this study, the earthquake catalog was originally developed by Ornthammarath et al (2011) [5]. This original catalog consists of instrumental earthquakes by Thai Meteorological Department (TMD), the USGS Determination of Epicenters on-line catalog, the International Seismological Centre (ISC), the US National Oceanic and Atmospheric Administration (NOAA), and the Global Centroid Moment Tensor catalogue, and the earthquake magnitude is reported using moment magnitude scale from 1912 to 2007. In current work, the catalog was updated by including additional events reported by Thai Meteorological Department (TMD) from 2008 to 2014, the USGS Determination of Epicenters on-line catalog, the International Seismological Centre (ISC), and ISC-GEM version 4 (1904-2014) (Di Gicamo et al., 2018) [7].

Different earthquake magnitude scales have been identified in the combined earthquake catalog. In order to homogenizing current earthquake catalog, all different earthquake magnitude scales are needed to be reported in the moment magnitude. The conversion is made using the magnitude conversion relations of Scordilis (2006) [8] from MS to MW, Sipkin (2003) [9] from mb to MW, and Heaton et al. (1986) [10] from ML to MW. Subsequently, duplicate events from different earthquake catalog were removed to create a processed earthquake catalog. The reaming number of processed catalog with unduplicated events shows 17,534 earthquake records with magnitude equal or greater than 3..

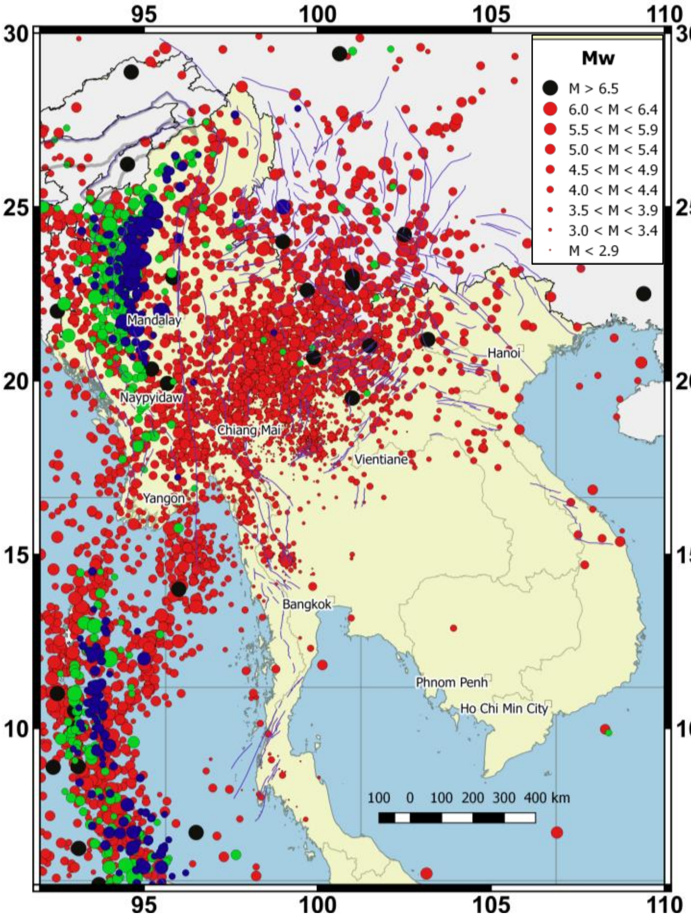

Figure 1. Northern South East Asia and its surrounding declustered earthquake catalog from 1905 to 2014. Shallow (depth < 50km) are shown in red circles, intermediate (50 < depth < 100 km) are shown in green circles, and deep (depth > 100 km) are shown in blue circles. Black circles represent shallow earthquake with Mw > 6.5.

3.DECLUSTERING

In addition, seismic hazard analysis is usually performed based on the Poisson distribution. The Poisson distribution assumes that occurrences of earthquakes are independent in time and that the dependent events such as aftershocks and foreshocks must be excluded from the earthquake catalog. Declustering process is usually performed to remove these dependent events. The earthquake catalog is divided into three-depth categories (i.e. 0 < depth < 50 km, 50 < depth < 100 km, and depth > 100 km) as described in the previous section due to different observed seismic activity rates as well as different wave propagation characteristic for ground motion models for the different tectonic regions to perform the seismic hazard analysis. Declustering procedure had been applied for different depth subsets of the catalog. This procedure eliminates about 62 percent of total events in the catalog. The declustered and processed catalog has 6,621 earthquake events in the Northern Southeast Asia region from 1905 to 2014, Figure 2.

4.CATALOG COMPLETENESS

The methodology to determine completeness periods for different magnitude ranges in current study is Stepp (1973) approache. In addition, the completeness analysis is performed for all seismic source models in current study. In total, seven seismic source models are considered based on different seismotectonic settings, variation in observed seismicity, and quality of available data. These zones including—3 subduction zones (SD-A, SD-B, and SD-C), which will be described in subduction zone section. For shallow earthquakes (depth < 50 km), two smooth seismicity models in Thailand (BG-1) and the remaining zone (BG-2) are delineated based on earthquake detection capacity. For intermediate (50 < depth < 100 km) (BG-Inter) and deep earthquakes (depth > 100 km) (BG-Deep), we considered to model only the intermediate and deep seismicity inside Myanmar subduction slab due to different seismicity rate compared to those Andaman trench. For each seismic source models, the completeness analysis is carried out independently. The results of Stepp (1973) approach for zones BG-1, BG-2, BG-Inter, BG-D, and subduction zones are presented in Table 1. These seven zones are shown in Figure 3 and 4

Table 1. Time periods of complete data and source parameters

Zone	Magnitude range	a	b	Completeness Intervals				
				$M_w \geq 5.0$	$M_w \geq 5.5$	$M_w \geq 6.0$	$M_w \geq 6.5$	$M_w \geq 7.0$
1 Background Seismicity								
BG-1	4.5 – 6.5	Smooth Seismicity	0.90	≥ 1972	≥ 1964	≥ 1930	≥ 1912	≥ 1912
BG-2	4.5 - 6.5		0.90	≥ 1972	≥ 1964	≥ 1930	≥ 1912	≥ 1912
BG-Inter	5.0 - 7.5		1.66	≥ 1975	≥ 1956	≥ 1931	≥ 1931	≥ 1931
BG-Deep	5.0 - 7.5		1.48	≥ 1973	≥ 1973	≥ 1956	≥ 1956	≥ 1956
2 Subduction Zone								
SD-A	6.5 - 8.5	5.85	1.02	≥ 1964	≥ 1962	≥ 1955	≥ 1925	≥ 1912
SD-B	6.5 - 9.2	5.49	0.95	≥ 1960	≥ 1950	≥ 1930	≥ 1925	≥ 1912
SD-C	6.5 - 9.2	5.52	1.08	≥ 1960	≥ 1950	≥ 1930	≥ 1925	≥ 1912

5.SMOOTH SEISMICITY MODEL

Smooth seismicity model has generally been considered to evaluate seismic hazard based on location of observed seismicity in the study region. In this study, the model accounts for all earthquakes within current study area with no active fault, and for smaller earthquakes in area with known active faults and subduction zone. The smooth seismicity methodology proposed by Frankel (1995) [12] has been utilized in this study. This method subdivided large zone to small grid, for our study a grid of 10 by 10 km2 is adopted, and the number of earthquake in each grid cell with magnitude greater than a threshold value seismicity rate is counting. Following Ornthammarath et al. (2011) [5] procedure, small earthquake data in BG-1 are much more completely recorded than other zones due to high earthquake detection capacity of TMD seismic network. Therefore, the estimated seismicity rate could be improved by including small earthquakes in hazard calculation. For BG-1 model, the smooth seismicity rate is determined based on particularly small earthquakes (moment magnitude > 3) detected by locally dense seismic network within Thailand. For this model, future moderate earthquakes believe to occur in area where high number of low to moderate tremors have been detected. In contrast, BG-2, BG-Inter, and BG-Deep models only determine smooth seismicity rate based on earthquake with moment magnitude greater than 5 since moderate seismicity in these zones are relatively high; thus, the rate can be reliably estimated from moderate-sized earthquakes.

Subsequently, the seismicity rate in each grid cell is determined by number of earthquakes dividing by the completeness year of earthquake data. Later on, computed rate is smoothed by using Gaussian smoothing by multiplying a Gaussian-function by the correlation distance C:

$$\overline{n}_i = \frac{\sum_i n_i e^{-\Delta_{ij}^2/c^2}}{\sum_i e^{-\Delta_{ij}^2/c^2}} \tag{1}$$

where n_i is normalized to preserve the total number of events. Δij is the distance between the i th and j th cells. The sum is taken over cells j within a distance of 3C of cell i. The b and Mmax values from the G-R earthquake frequency relationship are assumed to be a regional constant. The correlation distance, C, is set to 50 km for earthquake in BG-1, while for BG-2, BG-Inter, and BG-Deep, C is equal to 75 km. The correlation distance is determined based on Frankel (1995) [12] and it is similar to earthquake location uncertainties and spatial trends of observed seismicity.

For shallow smooth seismicity model (BG-1 and BG-2), the minimum earthquake magnitude greater than 4.5 will be computed while for intermediate and deep smooth seismicity model (BG-Inter and BG-D), minimum earthquake magnitude greater than 5.0 will be considered since smaller earthquake for intermediate and deep seismicity are less likely to cause moderate damage to structures. For maximum earthquake magnitude, both shallow smooth seismicity models are 6.5. This is due to the fact that, large earthquakes are already taken into accounted in causative fault modeling, which will be described in fault modeling section, and it is unlikely earthquake magnitude greater than 6.5 will go beyond these causative faults. In addition, to avoid double counting effect, a 'pure characteristic model' could be used where a GR model is used for small to moderate magnitudes and then a characteristic model for larger magnitudes on faults which is larger than the background seismicity Mmax (Stirling et al., 2012). For intermediate and deep seismicity (BG-Inter and BG-Deep), the maximum (upper bound) magnitude equals to 7.5, which is the largest reported earthquake plus 0.3 magnitude units. Both shallow seismicity models have the fixed depth at 7.5 km and the seismogenic layer extending between 5 and 15 km. For intermediate and deep seismicity models, the fixed depth equal to 75 and 125 km, respectively and the seismogenic layer extending between 50 and 100 km and between 100 and 150 km, respectively.

6.SUBDUCTION ZONE MODEL

In current study, three subduction zones are employed including: SD-A (the Myanmar subduction source zone), SD-B (the Northern Sumatra Andaman suduction source zone), and SD-C (the Southern Sumatra subduction source zone). These subduction zones are modeled to rupture along an angled plane right at the point of the interface between Indian-and Eurasia- tectonic plates, and Table 1 shows computed GR a- and b-values for each zone.

For each subduction zone, the minimum magnitude is 6.5, and for zone SD-A, SD-B, and SD-C, the maximum magnitude equals to 8.5, 9.2, and 9.2 respectively. For SD-A, this maximum magnitude is equal to the 1762 Arakan earthquake following the coastal net-uplift data as reported in Wang et al. (2014) [13]. However, for SD-B and SD-C, maximum magnitude for these subduction zones is similar to the size of the 2004 Sumatra earthquake. Each subduction zone is modeled to rupture from top (at 5 km) to bottom (at 50 km) as an inclined plane along plate boundary. Lastly, in order to estimate the rupture dimensions (i.e. length and width), the source scaling empirical formula for subduction interface earthquakes between moment magnitude and rupture area developed by Strasser et al. (2010) [14] are adopted for zone SD-A, SD-B, and SD-C.

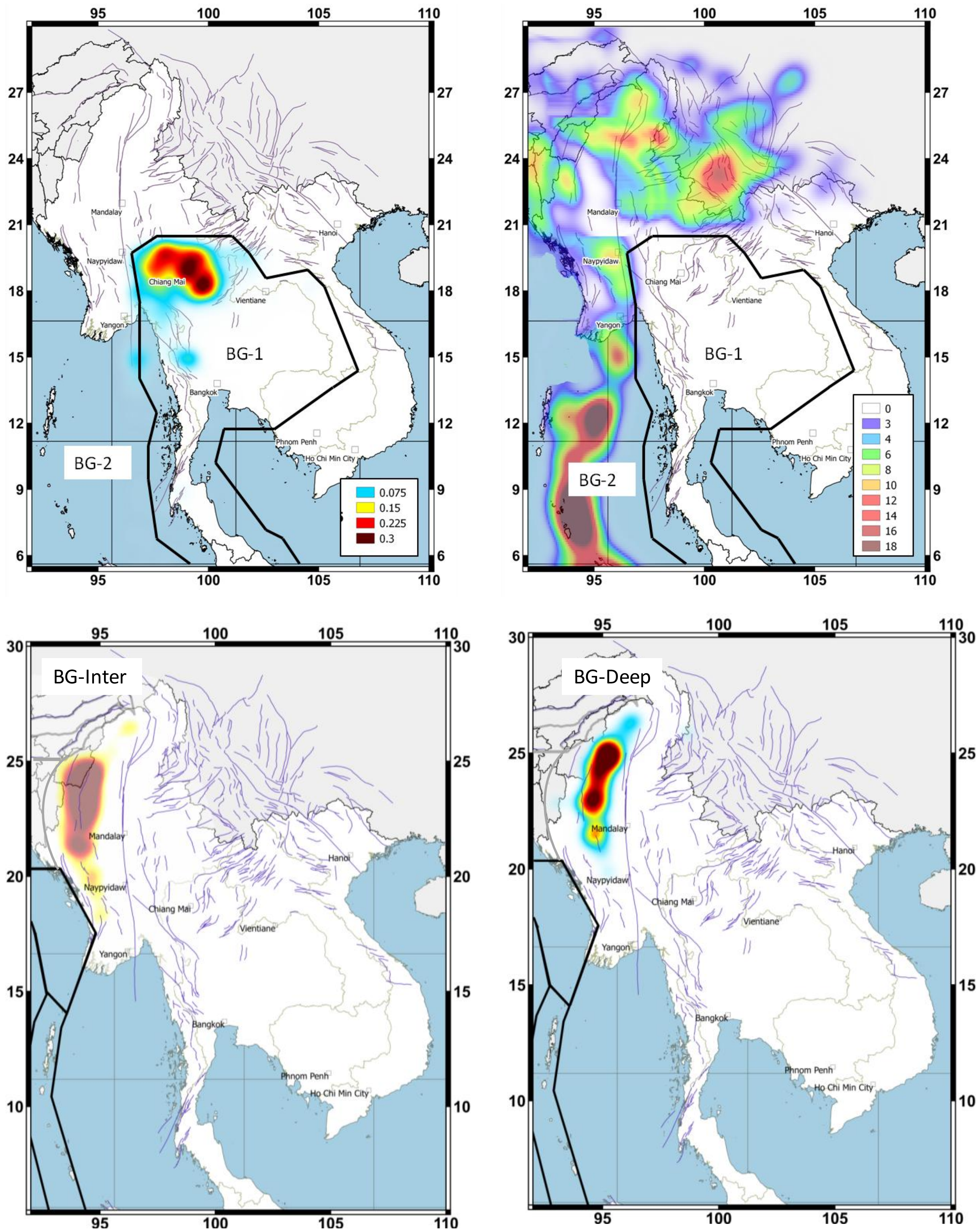

Figure 3. Smoothed seismicity rates of shallow events (0–50 km depth) inside BG-1 (Top left) and BG-2 (Top right), intermediate events (50–100 km depth) (BG-Inter) (Bottom left), and deep events (BG-deep) (greater than 100 km depth) (Bottom right) in the region. It can be clearly seen that the most active seismic sources are located along the active tectonic structures such as Sagaing fault, and secondary active faults

7.CRUSTAL FAULT SOURCE MODEL

Four hundred and twenty seven (427) crustal fault sources are modeled in this work as shown in Fig. 3. This active fault information has been reviewed and studied from recent paleoseismic investigation performed by several studies [13]. In addition, for onshore subduction interface, whose location could be clearly defined, is modeled as a complex fault as defined by depth contours based on Wang et al. (2013)' [13] s study. Moreover, discussions among our team members have been made through several meetings to review these fault parameters before implementing in our analysis. The fault parameters including in current database include slip rates, locations, dips, and upper and lower depths. In general, the strategy to assign slip rate for each fault is based on reliability of published studies. For example, if the results of studies are based on recent trenching investigations, those slip rates will be preferred instead of studies based on comparison of geomorphology. Their important properties and parameters with slip rate larger than 15 mm/year located within North Southeast Asia (NSA) are summarized in Table 2. For all considered faults in this study, the electronic supplements to this article, which contain all fault parameters, are also provided.

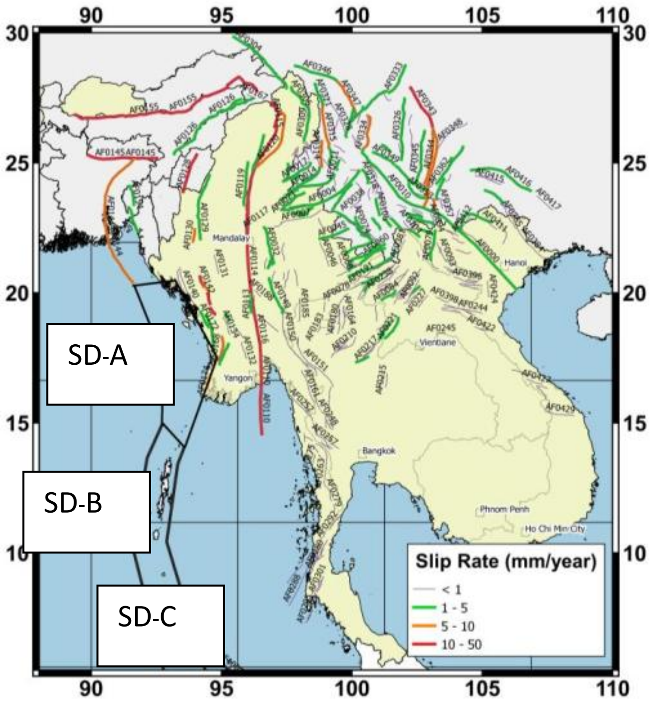

Figure 4. Faults and subduction zones considered in the NSAHM18 Seismogenic Faults database. Color-coded by slip rate (mm/y) are shown to illustrate the expected crustal movement rates. Red stars represent recent earthquakes with recorded ground motion discussing in current study. A yellow star represents the great 1762 Arakan earthquake with approximated epicentral location determined by Wang et al. (2013) [13].

To account for uncertainties in the modeling of these crustal faults, the logic tree method is employed in this PSHA study. The logic tree diagram of fault models is presented in Figure. 5. Similar logic tree diagrams are also made for the remaining faults.

Two assumptions are used to model earthquake recurrence behavior of these crustal faults: the characteristic earthquake and Gutenberg Richter models. Mmax is estimated from each fault length following the Wells and Coppersmith (1994) [15] relation. For subduction-zone earthquakes, the equation developed by Strasser et al. (2010) [14] is adopted for all considered onshore subduction interface. In addition, the regional b-value, 0.90, is assumed for each fault, and the earthquake activity rate is determined from seismic moment rate in order to assign a value for each fault. For characteristic earthquake model, epistemic uncertainty of maximum magnitude is considered by assigning three different magnitudes (Mmax - 0.2, Mmax, and Mmax + 0.2) with the logic tree weights of 0.2, 0.6, and 0.2, respectively. In addition, the earthquake recurrence interval is derived from where μ is modulus of rigidity, 3.0× 1011 dyne/cm2, A is area of the fault, is the assigned slip rate, MoC is the characteristic earthquake moment, which is derived from log (MoC) = 1.5 Mmax + 16.05. Moreover, the logic tree weight for both earthquake recurrence models is assumed to be equal (0.5 for characteristic and Gutenberg Richter models). This selected logic tree weight is similar to methodology adopted by Ornthammarath et al. (2011) [5]

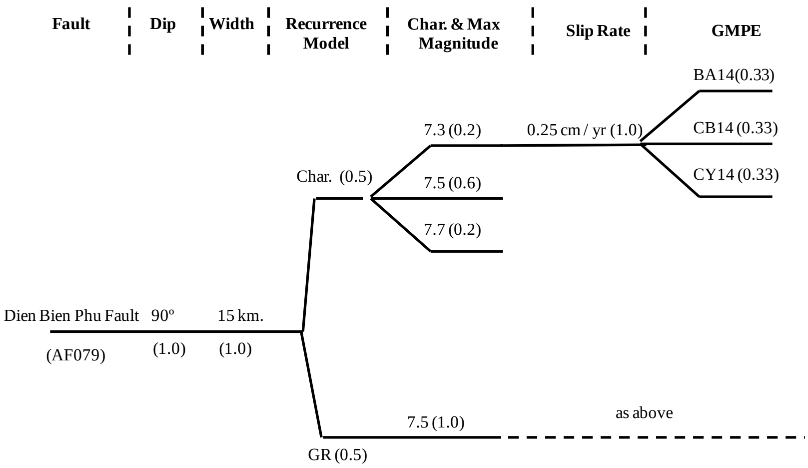

Figure 5. The Logic Tree for Dien Bien Phu fault source model in this work.

8.GROUND MOTION MODELS

For current study region, limited numbers of recorded ground motion are available since, as previously explained, the digital seismic networks for countries in NSA have just recently been implemented. Although, available strong ground motion data have been recorded by local seismic networks and compared with existing GMMs from three recent earthquakes in NSA with magnitude greater than 6.0 (i.e. March 24, 2011, Mw 6.8 Tarlay earthquake in Myanmar,; May 5, 2014, Mw 6.1 Mae Lao earthquake in Chiang Rai, Northern Thailand; and August 24, 2016, Mw 6.8 Chuak earthquake in Myanmar), there is still debate in our recent meetings regarding to their applicability for other parts in NSA where damaging ground motion has not yet been observed (e.g. southern Vietnam). However, at present, there is an agreement that the entire NSA should be considered as the same tectonic regionalization, and only existing GMMs developed for similar seismotectonic characteristics with rigorous database and assessment should be selected, while ongoing seismic monitoring will consider being an important issue to solve this problem in the coming future.

Table 2. Crustal fault source model parameters with slip rate larger than 15 mm/year located within North Southeast Asia (NSA).

Fault ID	Name	Length (km)	Characteristic earthquake magnitude			Slip rate (mm/yr)	Recurrence interval (yr)		
			Min	Mean	Max		Min	Mean	Max
110	Sagaing fault	385	7.9	8.1	8.3	20	197	392	783
112	Sagaing fault	86	7.1	7.3	7.5	15	95	189	376
114	Sagaing fault	238	7.6	7.8	8.0	20	142	283	565
115	Sagaing fault	114	7.3	7.5	7.7	15	172	343	685
116	Sagaing fault	120	7.3	7.5	7.7	20	89	178	355
117	Sagaing fault	381	7.9	8.1	8.3	18	217	433	865
118	Sagaing fault	73	7.0	7.2	7.4	18	106	212	422
124	Sagaing fault	65	7.0	7.2	7.4	18	97	194	388
125	Sagaing fault	64	7.0	7.2	7.4	18	97	193	385
128	Churachandpur-Mao Fault	168	7.5	7.7	7.9	16	419	836	1668
155	Himalayan frontal thrust	840	8.4	8.6	8.8	15	264	527	1051
343	Xiao Jiang	198	7.5	7.7	7.9	15	167	333	665

For current study, Campbell and Bozorgnia (2014) [16], Boore et al. (2014) [17], and Chiou and Youngs (2014) [18] are applied for active shallow region with equal logic tree weight including BG-1 and BG-2, and for active fault model. Comparison of recorded PGA and Spectral acceleration (T = 1.0 s) from recent earthquakes with NGA and NGA-W2 equations suggest that the chosen NGA-W2 GMMs provide relatively good fit with local data over the applicable distance range from 0 km to 200 km. Although there is a suggestion to include additional GMMs from other different databases, e.g. European and the Middle East), only selected NGA-W2 GMMs are considered because the current selected GMMs provide coefficients up until 10 second structural period which is the requirement of structural engineers.

To estimate ground motion for subduction interface GMMs in SD-A, SD-B and SD-C, we implement three subduction interface ground motion models. These GMMs are Atkinson and Boore (2003) [19], Abrahamson et al. 2016 [20](both of which are based on global data), and Zhao et al. (2006) [21](mostly based on data from Japan). Logic tree weights given to these GMMs are 0.10, 0.45, and 0.45, respectively. The Atkinson and Boore (2003; 2008) global model is retained with a lower weight because the possibility of gentle decay with distance of the intermediate- to long-period motion cannot be ruled out. No strong-motion data is available to guide the selection of GMMs for such earthquakes, but these models and their weight are comparable to the ones incorporating for such earthquakes in similar tectonic regions (Petersen et al, 2014). For intermediate- and deep- seismicity (50–100 km and > 100 km, respectively), we use Atkinson and Boore (2003) [19], Abrahamson et al. 2016[20], and Zhao et al. (2006) [21]empirical relations developed from intraslab earthquakes with 0.10, 0.45, and 0.45weight, respectively.

9.PROBABILISTIC SEISMIC HAZARD RESULTS

Lastly, the NSAHM18 hazard map is computed by the Open Quake engine. We present our results as mean PGA hazard maps for 475 and 2,475 year return periods, equivalent to 10 and 2% exceedance in 50 years, Figure. 6 a and b, respectively. The computed hazard map is performed on a reference rock site condition with an average shear wave velocity at 30 m top layer around 760m/s.

In general, western part of NSA has high seismic hazard relative to the east particularly along Sagaing fault where faults and smoothed seismicity both dominate to seismic hazard. The NSAHM18 hazard map for PGA at 475-year return period indicate high hazard along the fast slip rate Sagaing fault (PGA > 0.4g). Due to low slip rate faults in eastern Myanmar, northern Thailand, northern Laos, and northwest Vietnam, their contribution to seismic hazard is not obvious on this map. Moderate hazard level (0.1 g < PGA < 0.25g), at 475-year return period, then covers most parts of this region comparable to observed seismicity pattern (see Fig. 1). In contrast, the low slip rate faults become obvious in the 2475-year return period PGA map. Along the vicinity of modelled active faults, high ground motions could be clearly seen. These results verify the significance of further active fault research in this region.

Generally, the seismic hazard contour is comparable to those in past analysis; however, some dissimilarity is observed when comparing the estimated PGA from current work to previous studies. Notably, the estimated level of PGA near the border of Thailand, Lao PDR, Myanmar (generally known as Golden triangle area) (i.e. 0.4g) at 475-year return period, is about two times greater than the one described in GSHAP (Shedlock et al., 2000) [3]and Myo Thant et al., (2012) [4]. This observed difference is due to the fact that our model considering recent paleoseismic active fault data which had not been available or considered previously.

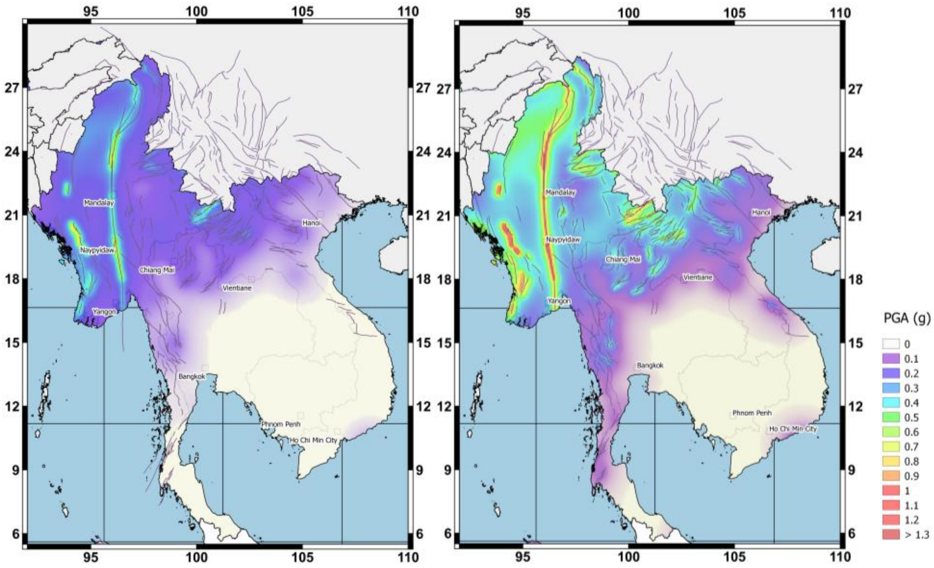

Figure 6. Probabilistic seismic hazard map for mean PGA at 10% and 2 % exceedance in 50 years.

10. CONCLUSION

Past PSHA maps in Northern Southeast Asia had previously been assessed [2-5] ; however, these maps have generally been constructed based on national level with limited consideration of nearby seismogenic sources. The current study represents PSHA map for this region since the Global Seismic Hazard Assessment Program (GSHAP) by Shedlock et al., 2000 [3]. The map is based on combination of smoothed gridded seismicity, crustal fault, and subduction zones. The smoothed gridded seismicity model is based on available seismicity data and could be separated into four sources (BG-1 & BG-2 for shallow depth, BG-Inter for intermediate depth, and BG-D for deep source). For crustal fault and subduction models, four hundred and twenty seven (427) crustal faults and three subduction zones had been reassessed and discussed regarding to their long-term slip rates and implication toward seismic hazard results. In addition, different ground motion models (GMMs) for three tectonic regions (Active Shallow Crust, Subduction Interface, and Subduction Intraslab) have been investigated and selected based on available recorded ground motion.

11. References

[1] Cornell CA 1968., Engineering seismic risk analysis. Bull Seism Soc Am 58(5):1583–1606.

[2] Phoung, N. H., 1991. Probabilistic assessment of earthquake hazard in Vietnam based on seismotectonic regionalization, Tectonophysics, 198, 81–93.

[3] Shedlock KM, Giardini D, Grünthal G, Zhang P, 2000. The GSHAP global seismic hazard map. Seismol Res Lett 71(6):679–689.

[4] Myo Thant., 2012. Seismic Sources Identification and Characterization for Myanmar: Towards Updating the Probabilistic Seismic Hazard Maps. AGU Fall meeting San Francisco, 14–18 December 2015.

[5] Ornthammarath, T., Warnitchai, P., Worakanchana, K., Zaman, S., Sigbjörnsson, R., and Lai, C. G., 2011. Probabilistic seismic hazard assessment for Thailand, Bulletin of Earthquake Engineering 9, 367–394..

[6] Chan, C.H. , Wang, Y., Shi, X., Ornthammarath, T., Warnitchai, P. Nguyen, P.H., Nguyen, L.M., Kosuwan, S., Thant, M., and Sieh. K., 2017., Toward Uniform Probabilistic Seismic Hazard Assessments for Northern Southeast Asia AGU Fall meeting San Francisco, 14–18 December 2015

[7] Di Giacomo, D., Engdahl, E. R., and Storchak, D. A., 2018. The ISC-GEM Earthquake Catalog (1904–2014):status after the Extension Project, Earth Syst.Sci.Data,10,1877-1899.

[8] Scordilis EM, 2006. Empirical global relations converting MS and mb to moment magnitude. J Seismol 10,225–236

[9] Sipkin SA, 2003. A correction to body-wave magnitude mb based on moment magnitude MW . Seismol Res Lett 74(6),739–742

[10] Heaton TH, Tajima F, Mori AW 1986, Estimating ground motions using recorded accelerograms. Surv Geophy 8, 25–83

[11] Stepp JC, 1973. Analysis of completeness of the earthquake sample in the Puget Sound area. In: Harding ST (ed) Seismic Zoning. NOAA Tech. Report ERL 267-ESL30, Boulder

[12] Frankel A 1995, Mapping seismic hazard in the Central and Eastern United States. Seismol Res Lett 66, 8–21

[13] Wang, Y., K. Sieh, S. T. Tun, K. Y. Lai, and T. Myint, 2014. Active tectonic and earthquake Myanmar region, J. Geophys. Res. 119, 3767–3822.

[14] StrasserFO, Arango MC, Bommer JJ. 2010 Scaling of the source dimensions of interface and intraslab subduction-zone earthquakes with moment magnitude. Seismol Res Lett 81, 941–950.

[15] Wells, D.L.and Coppersmith, K.J., 1994.New empirical relationships among magnitude, rupture length, rupture width, and surface displacements.Bull.Seism.Soc.Am.84 (4), 974-1002

[16] Campbell, K.W. and Bozorgnia, Y., 2014. NGA-West2 Ground Motion Model for the Average Horizontal Components of PGA, PGV, and 5% Damped Linear Acceleration Response Spectra. Earthquake Spectra: August 2014, Vol. 30, No. 3, pp. 1087-1115

[17] Boore, D. M., Stewart, J. P., Seyhan, E., and Atkinson, G. M., 2014. NGA-West 2 equations for predicting PGA, PGV, and 5%-damped PSA for shallow crustal earthquakes, Earthquake Spectra 31, 1057–1085.

[18] Chiou, B. and Youngs, R.R., 2014. Update of the Chiou and Youngs NGA Model for the Average Horizontal Component of Peak Ground Motion and Response Spectra.Earthquake Spectra: 2014, 30, 1117-1153

[19] Atkinson GM and Boore DM 2003, Empirical ground-motion relations for Subduction-zone earthquakes and their application to Cascadia and other regions. Bull Seism Soc Am 93,1703–1729

[20] Abrahamson, N., Gregor, N. and Addo, K., 2016. BC Hydro Ground Motion Prediction Equations for Subduction Earthquakes. Earthquake Spectra: 2016, 32, 23-44.

[21] Zhao JX, Zhang J, Asano A, Ohno Y, Oouchi T, Takahashi T, Ogawa H, Irikura K, Thio H, Somerville P, Fukushima Y, Fukushima Y ,2006. Attenuation relations of strong ground motion in Japan using site classification based on predominant period. Bull Seism Soc Am 96(3), 898–913

